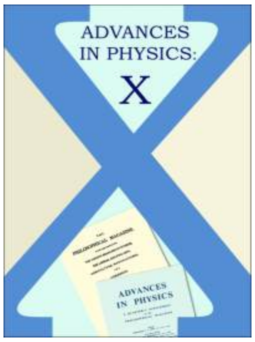

Advances in Physics: X

ISSN: 2374-6149 (Online) Journal homepage: www.tandfonline.com/journals/tapx20

Rainbow trapping for advanced wave control

Sayed El. Soliman, Maria Barlou, Kosmas L. Tsakmakidis & Zi Jing Wong

To cite this article: Sayed El. Soliman, Maria Barlou, Kosmas L. Tsakmakidis & Zi Jing Wong (2025) Rainbow trapping for advanced wave control, Advances in Physics: X, 10:1, 2517551, DOI: 10.1080/23746149.2025.2517551

To link to this article: https://doi.org/10.1080/23746149.2025.2517551

Published online: 18 Jun 2025.

ADVANCES IN PHYSICS: X
2025, VOL. 10, NO. 01, 1–31
https://doi.org/10.1080/23746149.2025.2517551

REVIEWS

OPEN ACCESS

Check for updates

Rainbow trapping for advanced wave control

Sayed El. Soliman[a,b], Maria Barlou[c], Kosmas L. Tsakmakidis[c] and Zi Jing Wong[a]

[a]School of Electronic Science and Technology, Eastern Institute of Technology, Ningbo, Zhejiang, China; [b]Physics Department, Faculty of Science, Assiut University, Assiut, Egypt and [c]Section of Condensed Matter Physics, National and Kapodistrian University of Athens, Athens, Greece

ABSTRACT

Rainbow trapping is a wave localization phenomenon in which different frequencies are spatially separated and confined by engineering dispersion through structural gradients. Initially demonstrated in tapered metamaterial systems, this concept has since been extended to plasmonic, photonic, acoustic, and elastic platforms, where graded-index profiles, chirped periodicities, and tapered geometries are used to control the group velocity and localize wave components at distinct spatial positions. These implementations enable high-resolution spectral manipulation and form the foundation for broadband wave control. More recently, topological rainbow trapping has emerged as a robust alternative, leveraging topologically protected states to achieve disorder-immune frequency localization. This approach offers enhanced resilience to fabrication imperfections and opens new possibilities for scalable, integrated wave-based devices. In this review, we examine the physical mechanisms, system-specific implementations, and recent advances in both conventional and topological rainbow trapping. We also highlight promising applications ranging from optical communication and wavelength multiplexing to acoustic wave manipulation and vibrational energy harvesting and discuss key challenges and future directions in this rapidly evolving field.

ARTICLE HISTORY
Received 14 February 2025
Accepted 4 June 2025

CONTACT Kosmas L. Tsakmakidis ktsakmakidis@phys.uoa.gr Section of Condensed Matter Physics, National and Kapodistrian University of Athens, Panepistimioupolis, Athens GR-157 84, Greece

GRAPHICAL ABSTRACT

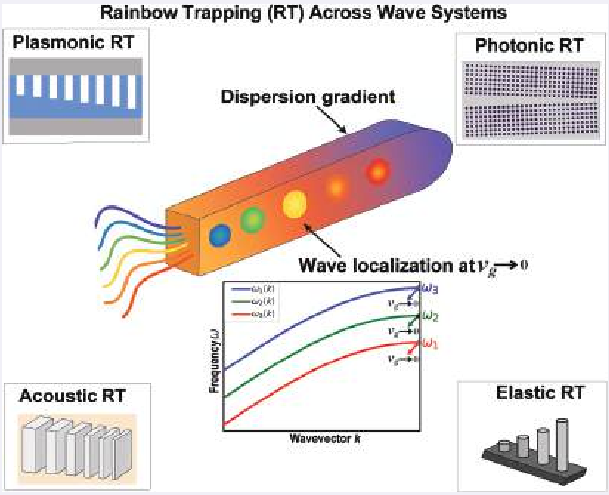

1. Introduction

Controlling wave dispersion is central to the manipulation of electromagnetic, acoustic, and elastic waves across diverse physical systems [1,2]. Among dispersion-based techniques, rainbow trapping enables spatial separation and localization of different wave frequencies through spatial gradients in structural or material properties [3–8]. These gradients include variations in refractive index, waveguide geometry, resonator dimensions, inter-element spacing, or mechanical stiffness, depending on the wave platform. By modulating the local dispersion relation, such gradients induce a gradual reduction in group velocity for each frequency component. When the group velocity ($v_g = d\omega/dk$) of a specific frequency approaches zero, that component becomes confined at a distinct spatial location, resulting in spatially resolved spectral localization, the hallmark of the rainbow trapping effect [9–18]. This phenomenon is governed by position-dependent dispersion and is achieved through adiabatic slowing in passive structures [19–27], without requiring time-dependent or externally driven modulation. Rainbow trapping thus enables broadband wave manipulation and underpins a range of applications in multiplexing, sensing, energy harvesting, and slow-light devices [28–30].

Rainbow trapping has been implemented across a wide range of physical platforms, including plasmonic systems [31–53], photonic crystal (PC) structures [54–59], acoustic media [60–66], elastic media [67–72], and topological systems [73–82], each leveraging spatial gradients to localize wave energy through dispersion tuning. In plasmonic rainbow trapping (PRT), surface plasmon polaritons (SPPs) are manipulated through engineered geometries to achieve frequency-selective light confinement. This is accomplished using graded grooves, tapered metal – insulator – metal (MIM) waveguides, hyperbolic metamaterials, or graphene-integrated gratings. These structures enable strong field confinement, subwavelength localization, and precise spectral control, making them particularly suited for high-resolution spectroscopy and optical buffering [46,83]. Photonic crystal rainbow trapping (PCRT) typically utilizes chirped or tapered periodic structures and gradient-index profiles to reshape the band structure and enable broadband light trapping, with demonstrated use in wavelength demultiplexing, dynamic frequency routing, and ultrafast light buffering [84–88]. In acoustic rainbow trapping (ART), spatial gradients in impedance or lattice spacing are used to slow and localize sound waves, often through graded-index metamaterials or coiled resonator arrays [89,90]. Elastic rainbow trapping (ERT), by contrast, involves structural variations such as graded stiffness, mass loading, or resonator height to confine mechanical vibrations at specific positions – commonly realized in notched beams or graded resonator arrays [91,92]. Both approaches are particularly suited for applications in energy harvesting and vibration control [93–95]. Despite differences in wave type and implementation, all platforms share the core principle of dispersion engineering through structural gradients to achieve frequency-dependent localization.

Conventional rainbow trapping structures, however, are susceptible to imperfections such as surface roughness, misalignments, or fabrication disorders, which can disrupt group velocity near the trapping point and significantly degrade performance [4]. To address these limitations, recent research has introduced the concept of topological rainbow trapping [96–103], which integrates rainbow trapping mechanisms with topologically protected states to achieve robust frequency-dependent localization [104–109]. These topological states arise at interfaces between regions with distinct topological phases [110–112] and exhibit confinement that remains stable against backscattering and fabrication variations [113–115]. By spatially varying interface geometry, lattice deformation, or coupling strength at the topological wall, the local dispersion of topological states can be tuned without altering the global topological phase, enabling frequency-selective localization along the interface [116–118]. Unlike conventional systems that rely on adiabatic slowing of bulk-guided modes, topological rainbow trapping manipulates the dispersion of pre-existing interface states, resulting in enhanced precision and robustness. This framework provides a compelling path toward scalable, high-performance wave-based devices capable of operating reliably under practical manufacturing conditions.

This review provides a comprehensive overview of the key physical mechanisms behind rainbow trapping across various wave systems. We discuss the physical principles of frequency-selective localization enabled by dispersion engineering and examine representative implementations in plasmonic, photonic, acoustic, and elastic platforms. Special attention is given to topological rainbow trapping, including its underlying physics and distinct advantages, particularly its robustness against structural imperfections and backscattering. We also highlight recent progress in mitigating energy dissipation and addressing scalability challenges, which are critical for real-world integration. Finally, we outline the diverse rainbow trapping applications, including optical communication, optical buffering, dynamic frequency routing, and energy harvesting. With its broad applicability, rainbow trapping is poised to become a foundational strategy for advanced wave control and the development of next-generation wave-based technologies.

2. Physical basis of rainbow trapping: a dispersion engineering framework

Rainbow trapping is, at its core, a manifestation of dispersion engineering, where the wave dispersion relation $\omega(k)$ is spatially tailored to control the group velocity v_g. This modulation causes waves of different frequencies to decelerate and become spatially localized at different positions along a structure, forming a 'rainbow' of confined frequencies. The principle is analogous to angular dispersion in a prism but is implemented via adiabatic slowing through structural gradients.

Two principal dispersion mechanisms govern rainbow trapping: Flat-band-induced trapping, where $v_g \to 0$ near a band edge (typically at $k = 0$ or $k = \pi/a$), as shown in Figure 1(a). Here, spatial gradients gradually shift the band structure until the operating frequency aligns with the flat region of the dispersion curve, resulting in strong field confinement [31]. This mechanism is prevalent in periodic systems (e.g. Bragg structures) or in waveguides with cutoff conditions (e.g. SPP). By adjusting parameters such as lattice spacing, refractive index contrast, or introducing localized resonators, the band flattening can be optimized for enhanced trapping efficiency and is well suited for broadband slow-light, sensing, and nonlinear enhancement. This spatial separation of frequencies forms the spectral 'rainbow' profile.

Inflection-point-induced trapping, where v_g vanishes at a turning point within the band (i.e. an inflection point), not at its edge as depicted in Figure 1(b). In this case, the curvature of $\omega(k)$ changes sign, causing waves to temporarily slow and reverse direction without permanent trapping [119,120]. The energy resides longer near the inflection point due to a local minimum in group velocity, offering a temporal delay and compact frequency routing. This mechanism, though resulting in weaker confinement, is useful for dynamic spectral control. It is often observed in systems involving resonant hybridization or coupled-mode dispersion. These two trapping mechanisms are not mutually exclusive and can often coexist within the same

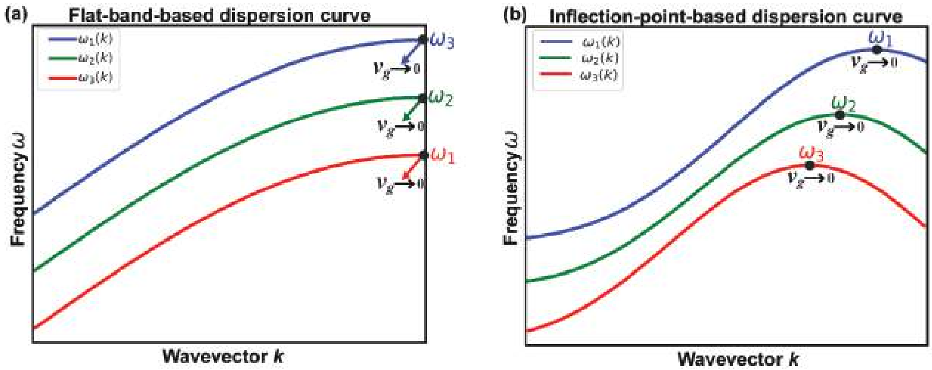

Figure 1. Dispersion engineering principles in rainbow trapping. (a) In flat-band-induced trapping, different frequency components experience vanishing group velocity near a band edge, leading to spectral localization and energy accumulation. (b) In inflection-point-induced trapping, the group velocity becomes zero at a turning point in the dispersion relation, enabling temporary localization and wave reversal but weaker confinement.

system. Design strategies such as tapering, chirping, or local modulation of unit cell geometry can be employed to tailor either type, depending on the application requirements.

Rainbow trapping is implemented differently across physical platforms. In plasmonic systems, SPPs exhibit strong geometry-dependent dispersion, enabling flat-band trapping through graded groove depths or widths. In photonic crystals, both mechanisms are accessible. Flat-band trapping occurs near photonic band edges using chirped periodicity or tapered waveguides. Inflection-point-based trapping arises in coupled-cavity arrays or Dirac-like dispersion regimes. In acoustic and elastic media, Bragg-type periodic structures yield flat-band trapping through spatially graded lattice parameters, while locally resonant metamaterials enable inflection-point slowing via graded stiffness, mass, or resonator spacing. Finally, in topological systems, wave localization emerges from topologically protected interface states rather than bulk band structures. However, even in these systems, the group velocity and frequency of edge or corner states can be spatially modulated via structural gradients, allowing rainbow trapping without altering the global topological phase. Depending on the structure, the dispersion of topological states may resemble flat-band or inflection-point profiles. Despite these differences, all systems exploit spatial dispersion shaping to achieve frequency-selective localization.

In this review, we distinguish three key structural concepts commonly used in rainbow trapping designs: graded-index (GI), chirped, and tapered. GI structures exhibit a continuous variation in effective refractive index or its analogs such as acoustic impedance or elastic modulus, along the wave propagation direction. Chirped structures involve a gradual change in periodic parameters, such as lattice spacing or resonator spacing, along the direction of propagation. Tapered structures feature smooth geometric variations transverse to the propagation direction, such as changes in waveguide width or resonator dimensions. Each approach modulates the local band structure to enable adiabatic slowing and frequency-selective localization through dispersion engineering. While these mechanisms are often combined in practice, we apply the terminology distinctly and consistently throughout this review.

3. Plasmonic and metamaterial rainbow trapping

Plasmonic rainbow trapping (PRT) exploits the dispersion properties of SPPs to achieve spatial separation and confinement of optical frequencies. In this implementation, the variations in geometry, such as groove depth, width, material gain, or resonator geometry, modulate the effective refractive index and shift the SPP cutoff frequency spatially, which enables precise control of group velocity. Accordingly, different frequencies are trapped at different positions, producing a nanoscale 'rainbow' of confined light.

GI structures form the foundation of many rainbow trapping systems, using spatial variations in refractive index to manipulate light. These platforms are especially valuable for high-resolution spectroscopy, optical buffering, and nonlinear optical devices. Gan, Ding et al. [31] presented one of the earliest demonstrations of PRT using a grating waveguide with a groove depth gradient from 140 to 230 nm. Simulations revealed multi-wavelength confinement from 1.33 to 1.65 *m*, with each wavelength localized where the group velocity approached zero near the cutoff, establishing the basis for geometry-induced SPP control (Figure 2(a)). Wang, Lu et al. [32] further enhanced tapered MIM waveguides by incorporating gain materials to compensate for losses. Group velocity was reduced below 0.01*c*, and near-complete light trapping was observed when gain matched the intrinsic absorption, demonstrating the feasibility of ultracompact slow-light buffers. Montazeri, Fang, et al. [33] presented a unique method via gradient groove-width for broadband PRT (Figure 2(b)). Their theoretical and numerical analyses revealed that sub-150 nm grooves enable broadband visible-range trapping through strong intragroove field coupling, while also simplifying fabrication compared to depth grading, making the approach practical for spectroscopic and sensing applications. Liu, Kanyang, et al. [53] extended these principles to highly doped silicon gratings, which provide long oscillation lifetimes of light trapping, enhancing slow-light effects for compact optical buffers and nonlinear optics. For typical GI structures, Dixon, Montazeri, et al. [34] provided a framework for fast, versatile analytical design and facile fabrication of ultrathin rectangular nanogrooves, structured into rainbow trapping arrays. Using Fabry – Perot modeling and simulations, they

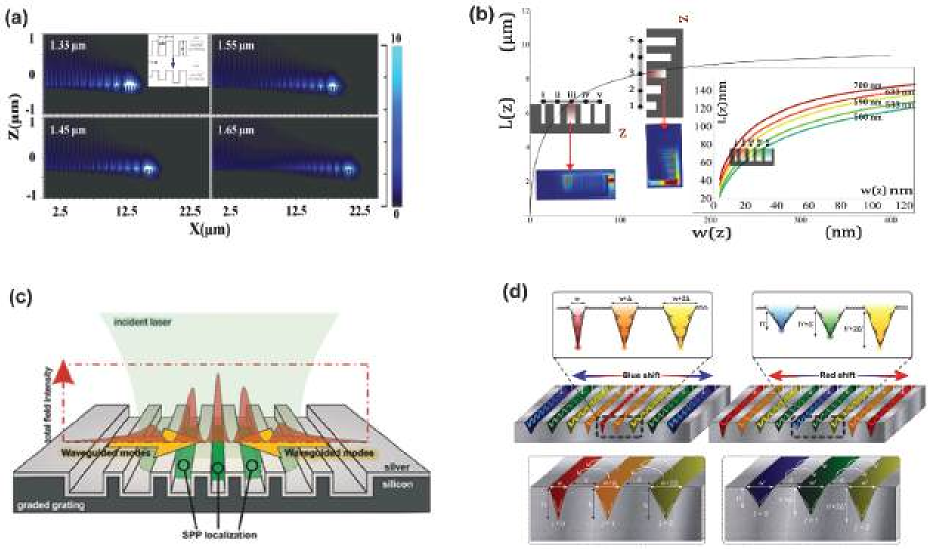

Figure 2. Gradient-based plasmonic rainbow trapping platforms utilize spatial geometric modulation for spectral localization. (a) Simulated electric field distributions $|E_z|$ at wavelengths $\lambda = 1.33,\ 1.45,\ 1.55, and 1mu 1.65\ \mu m$ in a metallic grating waveguide with groove depth graded from 140 to 230 nm. Each wavelength is trapped at a different spatial location due to groove-depth-induced cutoff shifts, where the group velocity approaches zero near the trapping point [31]. (b) Schematic of gradient groove profiles (left) and simulated dispersion curves for various groove widths (right). Each incident wavelength $(700500\ nm)$ is localized at a different spatial position along the grating, demonstrating broadband visible-range rainbow trapping [33]. (c) Width-graded metallic grating designed for multi-wavelength surface-enhanced Raman spectroscopy (SERS). Simulated field maps show spatial localization for different excitation wavelengths (532, 638, and 785 nm), with local field enhancements in the range of $10^6 - 10^7$ [35]. (d) Graded triangular groove array with depth and width modulation, supporting adiabatic energy transfer between grooves. SERS measurements reveal strong near-field localization and enhancement factors up to 8.5×10^9 under 532 nm excitation [36].

demonstrated local field enhancements near 10^3 and validated spectral confinement through far-field hyperspectral microscopy, confirming the design's suitability for broadband nanoplasmonic platforms.

For innovative GI designs, Liu, Wang, et al. [49] combined gratings with thermo-optic tuning to dynamically control trapping and releasing mechanisms. Their approach used index gradients induced by controlled temperature fields, enabling reconfigurable modulation suitable for integrated delay lines. The study by Zanjani, Shayegannia, et al. [35] leveraged PRT for multispectral surface-enhanced Raman spectroscopy (SERS). The system enhances Raman signal intensity over a broad spectral range by confining different wavelengths to distinct spatial locations, as shown in Figure 2(c). It demonstrated SERS enhancement factors up to 10^7 across 532, 638, and 785 nm lasers under practical fluidic conditions, confirming real-time spectral trapping. Zeineddine, Shayegannia, et al. [36] recently introduced graded triangular nano-gratings as an alternative to rectangular geometries for superior

SERS efficiency. The graded gratings allow the adiabatic transformation of SPPs, reducing losses and enhancing nanofocus across a broad spectrum, as shown in Figure 2(d). Their structure achieved up to 8.5×10^9 enhancement factors and consistent performance at visible wavelengths, particularly 532 nm, supporting broader optical sensing applications.

Beyond passive geometric grading, several advanced rainbow trapping platforms have emerged to expand functionality, tunability, and operational bandwidth. These include nonreciprocal systems, graphene-based waveguides, metasurfaces, and metamaterials, each introducing distinct physical mechanisms such as dynamic modulation or nonlinear response to further enhance light confinement. Nonreciprocal waveguides realize unidirectional trapping by time-reversal symmetry breaking. Liu and He [37] demonstrated trapped rainbows using a nonreciprocal waveguide under a tapered external magnetic field, offering robust wave localization even with fabrication disorders. The concept relies on asymmetric dispersion relations by incorporating gyromagnetic materials or external magnetic fields (Figure 3(a)). Simulations revealed long-lived hotspots and disorder immunity, highlighting a scalable route for robust light confinement. Graphene-based PRT platforms offer dynamically tunable slow-light effects in the mid-infrared. Yin, Zhang, et al. [52] demonstrated adiabatic control of dispersion curves in a silica – graphene – silica configuration. Here, air-gap modulation tunes the equivalent permittivity, enabling position-specific frequency localization through purely theoretical modeling. The study by Lu, Zeng, et al. [38] leveraged graphene's tunable plasmonic properties to achieve high slowdown factors for SPPs. The system consists of graphene monolayers on silicon-based graded gratings, with tuning enabled via gate voltage. Their design reached a slowdown factor of $\sim$450 and a $\sim$2.1 m bandwidth in a compact subwavelength platform. Ghaderian and Habibzadeh-Sharif [39] focused on graphene-based waveguides integrated with graded silicon gratings. High tunability is achieved via the chemical potential control of graphene, offering a slowdown factor of 1270 and a trapping bandwidth of 3.5 m (Figure 3(b)). Their gradient design in graphene – SiO – Si structure represents one of the most tunable mid-infrared PRT systems suitable for dynamic optical storage, high-speed optical switches, and mid-infrared sensing. Xu, Shi, et al. [40] introduced gradient metasurfaces designed with split-ring resonators (SRRs) to improve the oscillation lifetimes of trapped waves. Their experimental results confirmed long-lifetime resonance modes and spatial confinement via magnetoinductive channel coupling, enabling applications in multiplexing and optical filtering.

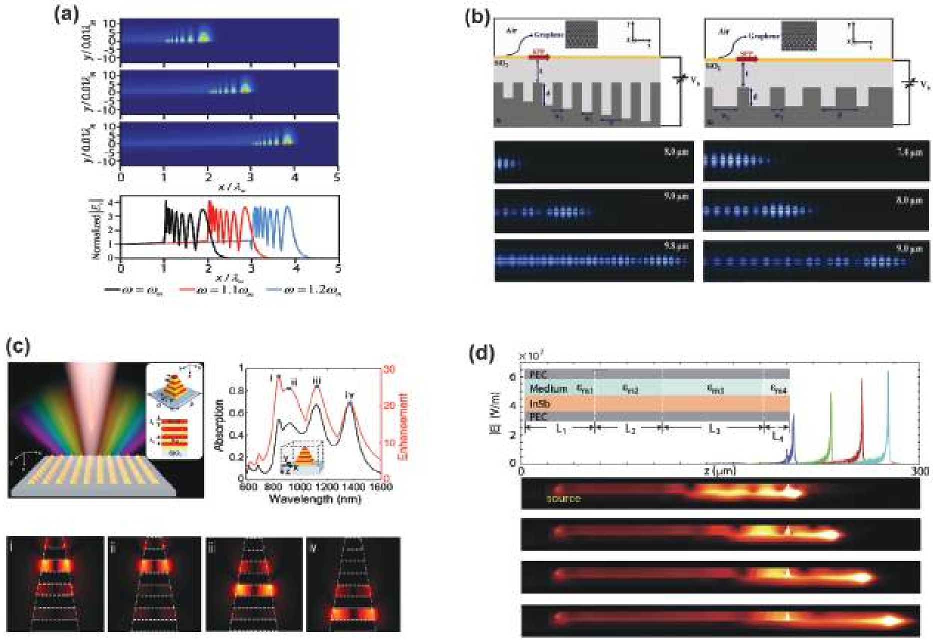

Figure 3. Advanced and tunable rainbow trapping platforms utilizing nonreciprocity effects, graphene tunability, and metamaterial dispersion engineering for broadband, dynamic, and directional spectral localization. (a) Simulated electric field distributions $|E_z|$ at different normalized angular frequencies ($\omega = \omega_0$, $1.1\omega_0$, and $1.2\omega_0$) for a nonreciprocal waveguide. The tapered magnetic field applied to a yttrium–iron–garnet (YIG) substrate induces asymmetric dispersion, enabling unidirectional rainbow trapping and long-duration hotspot confinement [37]. (b) Graphene–*Si* grating waveguide featuring graded groove width and depth, with simulated electric field profiles at three mid-infrared wavelengths. Modulating the chemical potential allows dynamic dispersion tuning, achieving slowdown factors exceeding 1270 and a spectral trapping bandwidth of 3.5 *m* [39]. (c) Hyperbolic metamaterial (HMM)-based structure formed from alternating Au/ZnO layers. The design supports full-color second harmonic generation (SHG), with electric field maps for visible excitation $(470-650\,\text{nm})$ and SHG spectra showing conversion efficiencies up to 1.13×10^6 and enhancement factors exceeding 50 using only 8.8 mW input power [41]. (d) Schematic and simulation of a one-way THz waveguide composed of epsilon-negative (ENG) and epsilon-near-zero (ENZ) metamaterials bounded by perfect magnetic conductors (PMCs). The resulting exhibits strong field confinement, and directional transport [42].

Metamaterials offer engineered subwavelength structures to manipulate wave propagation, excelling in nonlinear optics, compact device integration, and high-density optical storage. Hu, Ji, et al. [48] proposed a hyperbolic metamaterial (HMM) design that overcomes the limitations of traditional IMI or MIM waveguides by leveraging hyperboloid iso-frequency surfaces to enhance photon harvesting and light-matter interactions. Li, Hu, et al. [41] extended this concept for broadband second harmonic generation (SHG). Their Au/ZnO HMM design demonstrated field enhancement across $470-650\,\text{nm}$ and achieved SHG efficiencies over 1.13×10^{-6} with minimal input power, validating the potential of nonlinear PRT in ultrathin devices (Figure 3(c)). Xu, Xiao, et al. [42] presented broadband rainbow trapping using epsilon-negative (ENG) and epsilon-near-zero (ENZ) metamaterials. By coupling ENG/ENZ structures with perfect magnetic conductor boundaries, their waveguide achieved a threefold enhancement in trapping bandwidth and over five orders of magnitude in field intensification, supporting THz waveguiding and energy harvesting (Figure 3(d)). Zhao, Wu, et al. [121] recently introduced spatially confined HMMs that localize different wavelengths into ribbon-like patterns, enabling high field intensities across a broad spectrum for optical modulation and storage. Across diverse implementations, rainbow trapping has evolved from theoretical constructs to experimentally validated platforms, including gratings, graphene-based waveguides, and metamaterials, each advancing tunability, spectral coverage, and field confinement. Graphene-based systems offer dynamic mid-infrared control via electrostatic or chemical tuning, while metamaterials such as HMM and ENG media extend trapping into the visible and THz regimes, enabling broadband responses. Nonreciprocal architectures add unidirectional light confinement through asymmetric dispersion engineering. Despite these advances, key challenges persist in reducing plasmonic losses and simplifying fabrication, especially for complex 3D gradients. Future progress will hinge on optimizing the trade-offs between loss, tunability, bandwidth, and scalability, potentially through hybrid materials and multi-physics co-design.

4. Photonic crystal rainbow trapping

Photonic crystal rainbow trapping (PCRT) emerges from the interplay between Bragg scattering and engineered dispersion [54–58], enabling frequency-selective spatial confinement of light. This is typically realized using three structural strategies: graded-index configurations that modulate the effective refractive index along the propagation axis, chirped periodicities that vary lattice constants or cell dimensions, and tapered waveguides that induce local bandgaps through gradual width modulation. These dispersion-shaping techniques underpin slow-light enhancement [122–131], optical demultiplexing, and spatial light storage, as explored in the following studies.

For example, He, Wu, et al. [54] utilized the dynamic modulation of rainbow trapping in tapered PC waveguides. The structure was implemented using a low-symmetric dielectric lattice on a polystyrene substrate, and this effect is dynamically tuned using external voltage changes, leveraging the electro-optic effect, enabling controlled trapping and release of light. Simulations demonstrated selective confinement within a 5% bandwidth and showed the potential for active release of trapped modes (Figure 4(a)). Giden and Mahariq [55] proposed a GI PC waveguide designed to achieve wavelength demultiplexing. In their implementation, rod radii were adiabatically varied along the propagation axis, and the system operated in the visible regime (584 – 539 nm), using side drop channels to extract localized modes

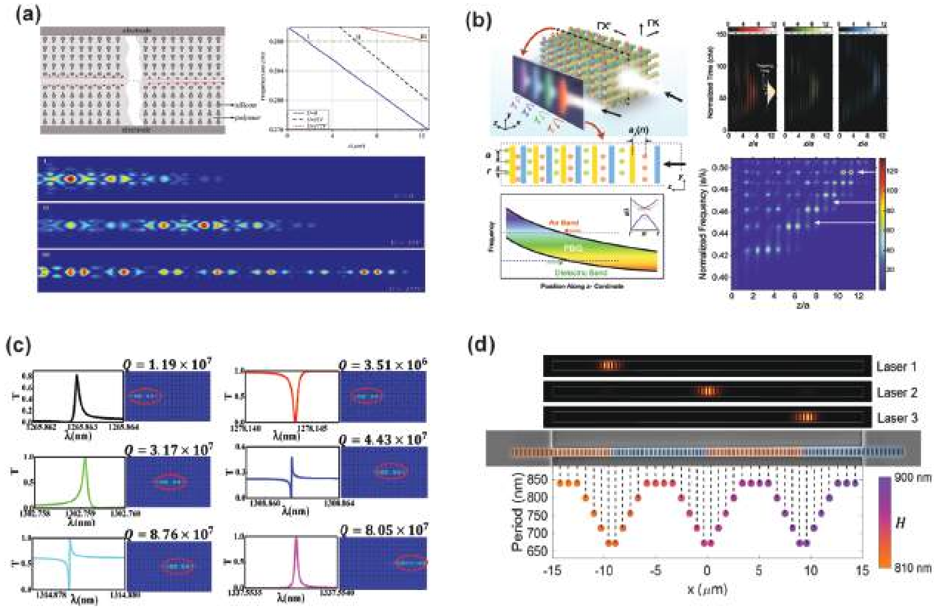

Figure 4. Photonic crystal rainbow trapping platforms utilizing dispersion-engineered structures. (a) Tapered electro-optic photonic crystal (PC) waveguide with voltage-controlled trapping. The top schematic shows a silicon–polymer hybrid waveguide with a gradually tapered PC region, modulated by applied voltages $U = 0$, 55 V, and 177 V. The right plot displays simulated spatial trapping positions at these voltages for an incident wavelength of 1.53 m, with the corresponding electric field $|E|$ distributions enabling electro-optic control of PCRT (bottom) [54]. (b) Chirped 3D woodpile PC for broadband rainbow trapping. The schematic illustrates a gradual variation in the layer-to-layer spacing along the z–axis, resulting in an adiabatically modulated photonic bandgap (left panels). Each frequency component is spatially trapped according to its position-dependent band alignment. The right panels show time-evolved field profiles of a Gaussian pulse and steady-state field distributions for three normalized frequencies $(a/\boldsymbol{\lambda} = 0.450,\ 0.468\ \mathit{and}\ 0.496)$ [56]. (c) Chirped semi-bilayer PC structure supporting ultra-high-Q Fano resonances. Transmission spectra and field distributions for multiple resonant modes demonstrate spatial separation and spectral selectivity, with Q-factors reaching up to 8.76×10^7 [58]. (d) Topological PC rainbow nanolaser. The top panel shows simulated electric field $|E|$ distributions for three lasing modes at 1550 nm, 1570 nm, and 1590 nm, each confined in a distinct topological cavity. The middle image is an SEM micrograph of the fabricated 1D topological laser, composed of alternating trivial (blue) and nontrivial (orange) photonic segments. The bottom schematic illustrates a variation in the lattice period a and height (H), inducing spatial dispersion gradient. This design enables wavelength-scale lasing with topological protection in the telecom band [73].

with high spectral resolution. The device achieved a compact footprint of 4.2 $m \times 2.8$ m and crosstalk as low as –30.6 dB, confirming its suitability for dense photonic integration. Similarly, Neşeli, Bor, et al. [57] developed a tapered 2D PC waveguide with integrated drop channels for wavelength division multiplexing. Four distinct wavelengths were extracted with coupling efficiencies of 75 – 80%, and experimental results matched simulations within 1% error. These findings confirm the effectiveness of localized mode-gap engineering for compact and reliable wavelength separation.

Chirped 3D PCs were demonstrated by Hayran, Kurt, et al. [56] using a woodpile structure with progressive interlayer spacing variation to enable spatial light confinement. This design produced a smooth transition in the local photonic bandgap, leading to the reflection and trapping of different wavelengths at specific spatial locations. The structure exhibited over two orders of magnitude in field enhancement and strong confinement in a defect-free bulk, validated both numerically and experimentally in the microwave regime (Figure 4(b)). Lastly, Soliman, Abood, et al. [58] developed a semi-bilayer PC structure that combines stacked lattices by engineering a chirped PC within the PCW to enable robust, multi-mode PCRT (Figure 4(c)). Their design spatially resolved three distinct resonant modes along the propagation axis, each supported by a separate Q-enhanced Fano state, allowing for simultaneous multiwavelength confinement with strong immunity to structural defects. This configuration is well-suited for compact and tunable photonic demultiplexers.

A key distinction between conventional and topological rainbow trapping lies in the spectral origin and spatial evolution of the supported modes. In conventional systems, spatial gradients adiabatically reshape the local band structure, gradually shifting guided modes derived from bulk bands into the bandgap. As the group velocity v_g decreases continuously along the propagation axis, different frequencies become localized at different positions (e.g. where $v_g \rightarrow 0$). The trapped field at each point thus remains part of an adiabatically evolved bulk mode. This process yields a smooth, continuous dispersion landscape and enables classical rainbow trapping via continuous frequency – position mapping.

In contrast, topological systems support discrete topologically protected states that emerge abruptly due to band inversion or symmetry-breaking transitions between adjacent regions with distinct topological invariants (e.g. Zak phases, Chern numbers) [118,132–136]. These states do not evolve from bulk modes; rather, they appear at domain walls. Their dispersion curves are confined to the bandgap and spectrally isolated from the bulk bands. Rainbow trapping in such systems is achieved not by forming new modes through gradients, but by modulating the dispersion of pre-existing edge states, shifting their group velocity and spatial localization via an applied gradient. This enables frequency separation through discrete mode redistribution, rather than the adiabatic evolution of bulk-guided modes. This behavior is well captured by the topological Hamiltonian formalism [137–139], commonly written as:

$$H(k) = d_x(k)\,\sigma_x + d_y(k)\,\sigma_y + d_z(k)\,\sigma_z,$$

$H(k)$ is the Bloch Hamiltonian as a function of wavevector k. $d_x(k)$, $d_y(k)$, and $d_z(k)$ are momentum-dependent coefficients, and σ_x, σ_y, and σ_z are Pauli matrices representing pseudospin degrees of freedom. A topological transition occurs when $d_z(k)$ changes sign across a domain wall signaling a change in the system's topological invariant. This inversion opens a bulk gap and guarantees the emergence of localized edge modes at the interface due to the bulk – boundary correspondence. Although the dispersion relation $\omega(k)$ remains mathematically continuous, the transition from extended bulk states to spatially confined edge modes is abrupt. This spectral reorganization, while continuous in energy-momentum space, appears discontinuous in real space.

Recently, Tian, Wang, et al. [73] demonstrated an ultra-compact topological PC rainbow nanolaser operating at the telecom wavelength of 1550 nm (Figure 4(d)). By engineering Zak phases and gradually varying unit cell dimensions, they achieved 64 spatially separated lasing peaks within a 0.002 mm footprint, with mode volumes as small as $\sim 0.7\,(\lambda/n)$ and spectral tuning spanning over 70 nm. The topological rainbow trapping mechanism enables robust, defect-tolerant light confinement within nanoscale cavities, making this architecture well-suited for high-density photonic chips and wavelength-scalable light sources in optical communication systems. In summary, PCRT designs have evolved from passive gradient-based structures to actively tunable and topologically robust platforms supporting functions such as demultiplexing and nanolasing. Despite these advancements, most devices still operate within narrow spectral bands, particularly in 3D or topological systems, and remain limited by fabrication and material challenges. Additionally, tight tolerances in semi-bilayer and chirped 3D architectures hinder repeatability and large-scale integration.

5. Acoustic rainbow trapping

Acoustic Rainbow Trapping (ART) refers to the selective confinement of sound waves by frequency at distinct spatial positions within engineered structures [66,90]. This phenomenon offers wide applicability in sound manipulation such as acoustic filtering, energy concentration, ultrasound imaging, and noise mitigation. For example, Zhu, Chen, et al. [60] numerically and experimentally demonstrated ART in a brass-based metamaterial composed of 80 subwavelength grooves with linearly varying depths (Figure 5(a)). Frequencies between 5 and 9 kHz were spatially trapped, with simulation and experiment confirming position-dependent localization and broadband spectral resolution. Similarly, Ni, Wu, et al. [89] and Lee, Jang, et al. [61] utilized coiled acoustic metamaterials to achieve compact multiband ART. The latter designed a coiled meta-silencer combining acoustic black hole (ABH) effects and rainbow trapping. Their structure, which includes a horn-like neck and a cavity, achieved a sound transmission loss spectrum across 200 – 1800 Hz. Six resonance peaks $(M_1$ to $M_6)$ are identified. Corresponding

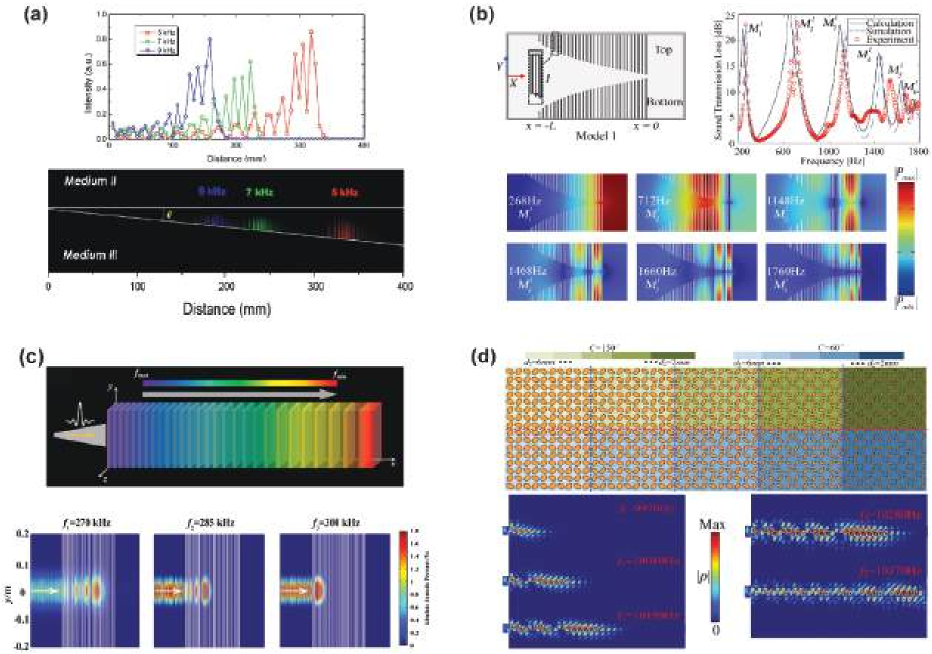

Figure 5. Acoustic rainbow trapping platforms utilize graded impedance, coiled geometries, and topological configurations. (a) Broadband rainbow trapping is achieved through groove depth grading in a brass-based metamaterial. The top panel shows calculated intensity profiles for discrete acoustic frequencies (5, 7, and 9 kHz), each trapped at a distinct location along the x–axis. The bottom panel displays simulated energy distributions in a structure composed of 80 subwavelength grooves with gradually varying depths, confirming broadband rainbow trapping [60]. (b) Compact coiled multi-slit acoustic black hole (ABH) structure exhibiting acoustic rainbow trapping. The left schematic depicts vertically arranged slits with gradually increasing lengths l, forming coiled ABH units. The right panel shows calculated, simulated, and experimental sound transmission loss spectra over 200–1800 Hz, identifying six resonance peaks $(M_1$ to $M_6)$. Corresponding pressure field maps illustrate efficient spatial localization of each resonant mode at 268, 712, 1148, 1468, 1660, and 1760 Hz [61]. (c) Gradient-index superlattices (GISLs) system enabling fluid-based rainbow trapping. The structure consists of stacked solid–fluid layers with progressively varying fluid thickness. Absolute acoustic pressure distributions reveal distinct spatial confinement of frequencies 270 – 300 kHz range, demonstrating broadband localization in a water-immersed configuration [62]. (d) Multidimensional topological acoustic rainbow trapping based on second-order topological sonic crystals. The top schematic shows a square lattice of elliptical cylinders with a gradient in short axis length, inducing edge states. Simulated acoustic pressure field distributions reveal distinct spatial confinement at different frequencies (9970, 10080, 10190, 10280, 10370 Hz), illustrating robust, defect-immune, multidimensional rainbow trapping [74].

pressure field maps validate efficient spatial trapping of each resonant mode for 268, 712, 1148, 1468, 1660 , and 1760 Hz as shown in Figure 5(b). This work emphasizes the advantage of compact broadband noise attenuation and efficient low-frequency sound absorption.

Zhao and Zhou proposed using microstructure metamaterials to achieve compact ART [64]. This vast technique includes creating miniaturized acoustic devices for portable sensors and medical diagnostics. In fluid media, Xu, Wu, et al. [62] introduced a gradient-index superlattice (GISL) composed of cascaded solid – fluid periodic layers to trap underwater acoustic waves. Their GISL broadened Bragg bandgaps and exhibited clear rainbow trapping in the 270 – 300 kHz range. Transmission spectra and finite element simulations using Gaussian beams showed high field localization and frequency separation, proving its potential for underwater sonar and sensing applications (Figure 5(c)). The concept has also been extended to topological acoustics, such as topological phononic crystals, which exhibit robust, defect-immune edge states that can guide sound waves along specific paths [140–143]. Chen, Yang, et al. [74] demonstrated a second-order topological sonic crystal structure capable of multidimensional rainbow trapping (Figure 5(d)). By gradually varying the short axis of elliptical scatterers in a square lattice, they achieved the spatial localization of both edge and corner states at distinct frequencies. Simulations revealed that topologically protected states are trapped without spectral overlap, highlighting robustness against defects. ART has progressed from early gradient-groove structures toward compact systems for targeted functions such as noise reduction, ultrasound imaging, and underwater acoustic sensing. The topological concentrators have the potential to be applied in high-precision acoustic sensing, energy harvesting. These developments reflect a shift toward miniaturized, broadband, and robust acoustic devices, though challenges remain in achieving real-time frequency control and broad operational tunability.

6. Elastic rainbow trapping

Elastic rainbow trapping (ERT) leverages spatial grading of mechanical properties to localize vibrational energy at frequency-dependent positions within a structure. ERT offers significant potential for applications such as energy harvesting, vibration control, and wave-based sensing. Graded resonator arrays are a common strategy to implement ERT. Arreola-Lucas, Báez, et al. [92] and De Ponti, Iorio, et al. [67] highlighted the role of graded arrays, such as notches in metallic beams or resonators, by altering the heights to reduce the wave group velocity. The latter demonstrated ERT using graded meta-waveguides, where the heights of resonators are progressively altered along the length of a beam. This structural gradient slows down incoming waves and traps them at spatial locations corresponding to their frequency. Experimental and numerical analyses showed that rainbow reflection and trapping occur due to either band-edge zero-group velocity or mode-locking. For instance, flexural waves are trapped depending on symmetry, with rainbow reflection leading to wave return and rainbow trapping enabling deep energy confinement, which is valuable for localized harvesting and mode conversion (Figure 6(a)). Meanwhile, Wang, Huang, et al. [68] investigated the integration of piezoelectric patches in a perforated metamaterial beam, where

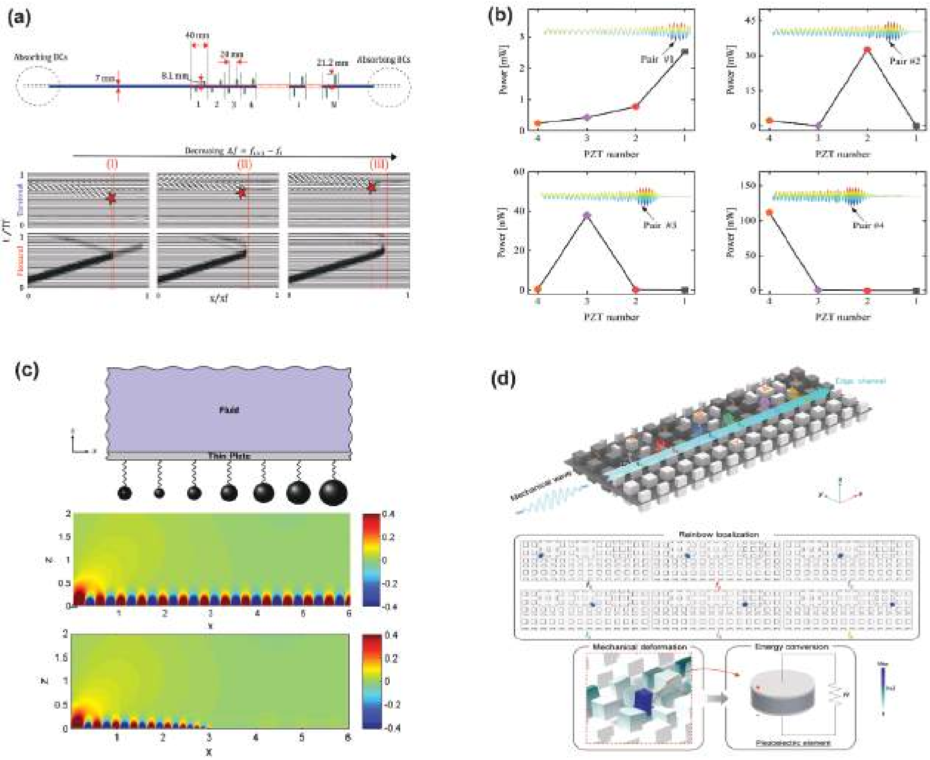

Figure 6. Elastic rainbow trapping platforms for vibration control, energy harvesting, and wave manipulation using graded resonant structures. (a) a graded array of asymmetric resonators with linearly increasing lengths (top panel). The bottom panels display space-time waterfall plots of vertical displacement (flexural) and the rotation (torsional) for increasing numbers of resonator pairs: (I) 9, (II) 25, and (III) 50. By increasing the number of graded resonators, i.e. from left to right, it is possible to move from locking to genuine rainbow trapping [67]. (b) The output power measurements from four pairs of piezoelectric patches correspond to distinct trapping frequencies: 27.7, 36.6, 44.8, and 53.4 kHz. Each subplot includes the spatial displacement field distribution in the metamaterial beam, demonstrating localized energy concentration at resonance positions [68]. (c) Elastic plate loaded by a fluid and augmented with a periodic array of graded mass–spring resonators (top). Time-harmonic pressure field snapshots (bottom) show the conversion of subsonic to supersonic waves and spatial separation of frequencies along the surface of the plate due to the graded configuration, enabling frequency-selective trapping [69]. (d) Schematics of the fabricated meta-device with piezoelectric patches at corner sites $C1-C6$ for energy harvesting (top). The conceptual diagram (bottom) illustrates how rainbow-localized mechanical deformations are converted into electrical energy through embedded piezoelectric elements. Multiple vibration modes are simultaneously trapped and harvested [75].

the local modification of wave dispersion enables multiple frequency energy harvesting by placing piezoelectric patches where wave localization arises, allowing for efficient mechanical-to-electrical-energy-conversion. Optimal harvesting performance was achieved in the 27 – 54 kHz range, with electrical output significantly enhanced when the resonance and trapping points coincide. These outcomes were supported by simulation and circuit-based output modeling (Figure 6(b)).

Furthermore, Alshaqaq, Sugino, et al. [71] demonstrated progress in forming tunable ERT by programmable metamaterials by adapting the inductive shunt frequencies in the piezoelectric array. This configuration enables real-time tuning of group velocity gradients, offering adaptive control over both energy localization and dispersion characteristics. In contrast, Chaplain, Pajer, et al. [93] analytically investigated the distinction between rainbow reflection and rainbow trapping in mass-loaded plates, offering theoretical clarity on how symmetry-breaking and modal coupling influence wave behavior. Finally, Skelton, Craster, et al. [69] created a multi-metawedge consisting of graded arrays on fluid-loaded elastic plates. This structure couples surface flexural waves with bulk acoustic waves, leading to mode conversion and rainbow trapping in underwater contexts. The system thus operates under elastic wave dynamics with additional acoustic coupling. The time-harmonic snapshot of pressure field plots reveals subsonic-to-supersonic wave conversion and frequency-selective trapping along the plate's surface due to graded geometry (Figure 6(c)). Topological ERT integrates structural grading with topologically protected states to achieve frequency-dependent wave localization, providing a robust energy confinement and manipulation mechanism [95,144]. Chen, Fan, et al. [75] proposed a high-order topological insulator structure using second-order phononic crystals that support multiple discrete states, enabling spatially selective confinement. Elastic vibrations propagate through the system coupled to edge-guided topological channels, which then trap energy at different engineered corner sites. The experimental setup showed robust energy trapping, enabling simultaneous multi-frequency energy harvesting using piezoelectric elements (Figure 6(d)). These investigations highlight the versatility of topological ERT for controlling mechanical waves and its potential to transform fields as energy harvesting and advanced waveguide design. ERT has evolved from static graded resonator arrays to multifunctional and topologically enhanced systems for precise vibrational energy localization. Key advances include the integration of piezoelectric harvesting, real-time tunable shunted metamaterials, and higher-order topological insulators for multi-frequency, defect-immune trapping. These studies collectively demonstrate the modulation of group velocity through structural gradients, enabling wave control for applications in energy conversion, vibration filtering, and intelligent mechanical systems, though challenges remain in broadband operation and fabrication scalability.

7. Addressing loss in real-world systems

In practical implementations of rainbow trapping, energy dissipation arising from intrinsic material absorption, scattering due to imperfections, and radiative leakage poses a major obstacle to confinement efficiency and overall device performance [3,126–128]. These effects are captured through a complex refractive index $n = n' + n''$, where the imaginary part n'' signifies attenuation. In such media, the electric field propagation along a lossy waveguide follows [79,98]: $E(z) = E_0.e^{-\alpha z}.e^{ikz}$ with α is proportional to n''. Higher n''values correspond to stronger attenuation, reducing the effective propagation length and trapping duration of localized modes. In topological rainbow trapping, while edge states are inherently robust to backscattering and certain forms of disorder, this immunity is not absolute. Excessive attenuation can shorten edge-state lifetimes, reduce propagation lengths, and in extreme cases collapse the bulk bandgap, effectively erasing topological protection. Moreover, thermal accumulation from absorption may even cause structural deformation or phase disruption.

To mitigate such effects, various complementary strategies have been developed. Material engineering focuses on low-loss platforms and engineered dielectrics with minimized absorption in the operational bandwidth [46,145]. In parallel, structural optimizations such as anti-reflection coatings, high-Q cavities, and impedance-matched interfaces help suppress scattering and radiative leakage. Systems with enlarged topological bandgaps further improve robustness by energetically isolating edge modes from bulk continuum states, thereby preserving topological characteristics even in dissipative conditions [135,146]. Another effective approach involves gain-assisted compensation. By redefining the refractive index as $n = n' + i(n'' - g)$, where g is a spatially engineered gain coefficient, dissipation can be selectively neutralized. Careful gain profiling allows tailored compensation that suppresses absorption without disturbing dispersion relations or topological invariants [147–149]. Beyond direct compensation, recent demonstrations of ultralow-loss performance via high-Q cavities and loss-engineered PCs show that device behavior can be significantly enhanced by optimizing the balance between confinement and dissipation [150–152]. In this context, non-Hermitian photonic design allows selective control over modal lifetimes and spectral features, supporting phenomena such as exceptional points and pseudo-Hermitian phase transitions [153,154]. Hybrid integration with low-loss platforms, including dielectric waveguides and fiber-coupled interfaces, offers another route to reduce propagation losses while maintaining functional confinement. These co-designed systems combine the strong localization capabilities of PCs with efficient transmission media to enable practical, broadband energy trapping [155–157].

Notably, alternative frameworks have demonstrated intrinsic resilience to loss without relying on complex structural gradients or compensation schemes. One such example involves the use of complex-frequency modes in uniform plasmonic heterostructures [5]. These modes, excited by time-dependent sources, exhibit weak leakage at their zero-point, thus supporting dispersionless light trapping without requiring a prism or extended propagation distance. Their evanescent spatial character minimizes interaction with surface roughness, particularly under grazing incidence, since energy is concentrated in the core of the mode, away from perturbations. This leads to enhanced tolerance against fabrication imperfections and opens new avenues for high-performance, broadband light confinement. Altogether, these approaches, spanning material innovations, topological bandgap engineering, gain profiling, non-Hermitian control, and hybrid integration, collectively converge to address the central challenge of loss in rainbow trapping systems. As these technologies mature, the prospect of realizing near-lossless, topologically robust, and highly confined wave localization becomes increasingly tangible, heralding transformative advances across photonics, acoustics, and elastic media.

8. Applications

Rainbow trapping enables precise spatial separation of wave components by frequency, unlocking diverse applications across diverse physical platforms. Engineering spatial dispersion profiles enables precise control for selective slowing, trapping, and release of waves, offering new functionalities in optical communication, ultrafast dynamic routing, and broadband energy harvesting.

8.1. Optical communication and wavelength division multiplexing

In optical communication, rainbow trapping provides a robust platform for wavelength separation and demultiplexing. By employing chirped PCs or GI structures, distinct spectral components are localized at different spatial positions, effectively reducing crosstalk and enhancing channel isolation. This enables high-fidelity operation in wavelength division multiplexing (WDM) systems where multiple data streams are transmitted through a single optical path. Localized bandgap formation in tapered PC waveguides allows specific wavelengths to be confined and extracted via integrated drop-channels with optimized coupling. As demonstrated in [57], tuning the dielectric rod positions in a tapered PCW can maximize the efficiency of wavelength drop-channels, achieving high transmission and low interference. Such devices are ideally suited for dense, high-speed optical networks (Figure 7(a)).

8.2. Ultrafast light buffering

Rainbow trapping also supports optical buffering through the engineered control of group velocity. Slow-light regions, where the group velocity approaches zero, can temporally delay optical pulses without distortion, functioning as passive delay lines [10,20]. When integrated with topological photonic structures, these buffers gain robustness to fabrication defects and backscattering, essential for fault-tolerant signal delay. Recent developments [158] demonstrate a compact, multistage delay line using topological detours, where delay increases linearly with detour number. This architecture supports broadband delays while preserving edge-state integrity, advancing optical memory and data synchronization technologies (Figure 7(b)).

8.3. Dynamic frequency routing

The growing demand for high-speed optical interconnects necessitates scalable solutions for routing different frequencies [159–162]. Rainbow trapping

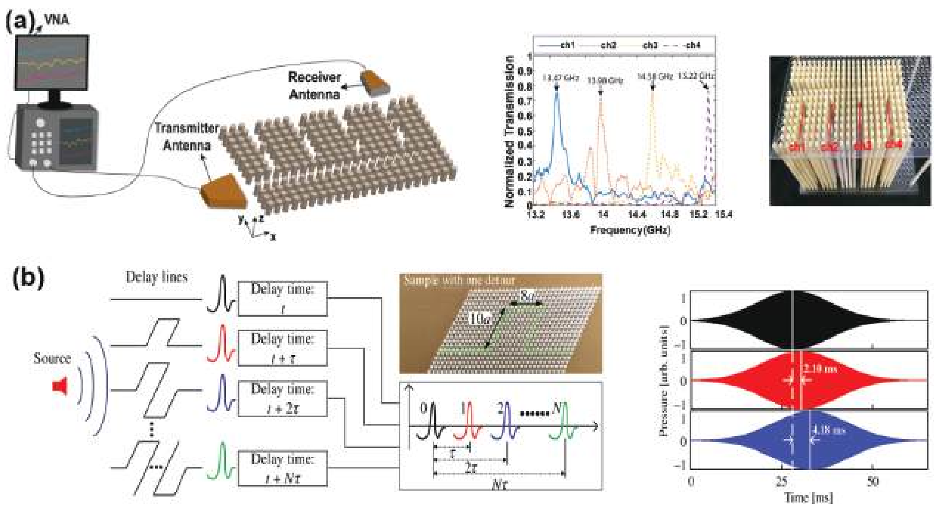

Figure 7. (a) Experimental setup and performance of a wavelength division multiplexing (WDM) photonic crystal (PC) system using rainbow trapping. The setup includes a transmitter and receiver antenna connected to a vector network analyzer (VNA), interfacing with a graded PC structure. The right panel shows the physical device and indicates the positions of the four drop-channels ($ch1-ch4$). The center panel presents the normalized transmission spectra for each channel, demonstrating wavelength-selective extraction at 13.47 GHz, 13.98 GHz, 14.58 GHz, and 15.22 GHz [57]. (b) Compact topological delay line based on engineered phase-delay detours (PDDs). The left schematic illustrates how input acoustic pulses are routed through delay lines with increasing detour length, generating progressive time delays t, $t+\tau$, $t+2\tau$, $t+N\tau$. The central panel shows the physical sample with one detour (lengths $8a$ and $10a$), where a is the lattice constant. The right panel displays the corresponding time–resolved pressure field measurements, revealing temporal delays of 2.10 ms and 4.18 ms for red and blue pulses, respectively, confirming scalable broadband acoustic delay [158].

enables frequency-selective routing by spatially modulating dispersion to steer specific wavelengths through predetermined paths. Topological photonic crystal waveguides (PCWs) support reconfigurable routing by modulating edge-state dispersion. In [88], a chirped topological PCW enabled real-time redirection of different frequencies via controllable sharp bends, preserving topological protection while dynamically rerouting signals, enabling broadband, adaptive routing in on-chip systems.

8.4. Highly efficient energy harvesting

Rainbow trapping extends to acoustics and elasticity, enabling broadband energy harvesting from ambient vibrations [93,94,163–165]. In such systems, graded elastic or acoustic metamaterials concentrate vibrational energy at specific locations. Piezoelectric elements placed at these trapping points convert mechanical energy into electricity over a broad frequency range [72,166,167]. The conversion efficiency is given by $\eta = P_{out}/P \times 100$, where P_{out} is the electrical output, and P is the acoustic input. By designing phononic crystals with dispersion gradients tuned to ambient vibration spectra, broadband acoustic energy harvesters can power sensors and embedded devices. Potential applications include powering low-energy devices via environmental vibrations, such as from pedestrian movement, traffic, or ocean waves. This offers a sustainable and distributed energy solution for smart infrastructure, autonomous sensors, and micro-power electronics.

Altogether, the spatial and spectral selectivity offered by rainbow trapping unlocks disruptive capabilities across domains, whether routing light on-chip, buffering ultrafast signals, or harvesting vibrational energy in noisy environments. These advances position rainbow trapping as a cornerstone for next-generation wave-based technologies.

9. Conclusion

Rainbow trapping has emerged as a powerful wave manipulation strategy, enabling frequency-selective confinement and spatial separation across diverse physical platforms. By tailoring the local dispersion relation through spatial gradients, it enables adiabatic slowing of wave packets and the localization of distinct spectral components at designated positions. This ability has unlocked a wide range of practical applications from optical multiplexing and buffering to energy harvesting and signal routing. Recent advances in topological rainbow trapping have addressed key limitations in conventional designs, particularly their susceptibility to backscattering, fabrication imperfections, and disorder. By leveraging topologically protected edge and corner states, these systems enable robust localization and transport immune to structural perturbation, an essential requirement for scalable, fault-tolerant technologies.

Despite the growing maturity of the field, challenges remain. Current implementations typically operate within limited spectral windows, constrained by material losses or narrow design bandwidths. Moving forward, expanded spectral coverage will depend on engineering wideband dispersion profiles through optimized structural geometries or novel materials. In parallel, integrating rainbow trapping with nonlinear optics, quantum photonics, or plasmonic nanostructures promise enhanced functionality. Nonlinear interactions could enable dynamic frequency control, while quantum topological states offer robust pathways for entanglement-preserving operations. Plasmonic topological platforms may further shrink device footprints while retaining high confinement.

Looking ahead, emerging approaches based on moiré-engineered flat bands provide new opportunities for extreme light confinement and novel slow-light phenomena, offering a compelling direction for future rainbow trapping implementations. Recent breakthroughs in magic-angle nanostructures have demonstrated stopped-light nanolasing, subwavelength mode volumes, and reconfigurable coherent emission arrays through interlayer-twisted photonic graphene lattices [168–171]. These systems achieve flat-band-induced localization via engineered mode coupling without requiring conventional bandgaps. To realize rainbow trapping in such platforms, spatial variation of the twist angle, interlayer coupling (e.g. via vertical separation or refractive index contrast), or unit cell registry can be used to introduce gradients in the flat-band condition. These variations enable frequency-dependent localization across the structure, forming a moiré-engineered analog to traditional graded-index or chirped periodic systems. This pathway opens up novel strategies for dispersion engineering and spectral separation in next-generation nanophotonic devices.

In summary, rainbow trapping, both conventional and topological, continues to evolve as a foundational tool for advanced wave control. With its deep physical roots in dispersion engineering and its rapidly expanding technological impact, it holds strong promises for driving innovation in communication, energy, and sensing systems. Ongoing progress in loss mitigation, topological robustness, and broadband design will be pivotal in transitioning rainbow trapping from laboratory prototypes to real-world applications.

Disclosure statement

No potential conflict of interest was reported by the author(s).

References

[1] Hau LV, Harris SE, Dutton Z, et al. Light speed reduction to 17 metres per second in an ultracold atomic gas. Nature. 1999;397:594–598. doi: 10.1038/17561

[2] Boyd RW, Gauthier DJ. Controlling the velocity of light pulses. Science. 2009;326:1074–1077. doi: 10.1126/science.1170885
[3] Tsakmakidis KL, Boardman AD, Hess O. 'Trapped rainbow' storage of light in metamaterials. Nature. 2007;450:397–401. doi: 10.1038/nature06285
[4] Tsakmakidis KL, Hess O, Boyd RW, et al. Ultraslow waves on the nanoscale. Science. 2017;358: p. eaan 5196. doi: 10.1126/science.aan5196
[5] Tsakmakidis KL, Pickering TW, Hamm JM, et al. Completely stopped and dispersionless light in plasmonic waveguides. Phys Rev Lett. 2014;112:167401. doi: 10.1103/PhysRevLett.112.167401
[6] Tsakmakidis KL, Klaedtke A, Aryal DP, et al. Single-mode operation in the slow-light regime using oscillatory waves in generalized left-handed heterostructures. Appl Phys Lett. 2006;89. doi: 10.1063/1.2387873
[7] Tsakmakidis KL, Hermann C, Klaedtke A, et al. Surface plasmon polaritons in generalized slab heterostructures with negative permittivity and permeability. Phys Rev B. 2006;73:085104. doi: 10.1103/PhysRevB.73.085104
[8] Gan Q, Fu Z, Ding YJ, et al. Ultrawide-bandwidth slow-light system based on THz plasmonic graded metallic grating structures. Phys Rev Lett. 2008;100:256803. doi: 10.1103/PhysRevLett.100.256803
[9] Chen J, Liang W, Li Z-Y. Switchable slow light rainbow trapping and releasing in strongly coupling topological photonic systems. Photon Res. 2019;7:1075–1080. doi: 10.1364/PRJ.7.001075
[10] Elshahat S, Wang C, Zhang H, et al. Perspective on the topological rainbow. Appl Phys Lett. 2021;119:230505. doi: 10.1063/5.0074014
[11] Shen Y, Fu J, Yu G. Rainbow trapping in one-dimensional chirped photonic crystals composed of alternating dielectric slabs. Phys Lett A. 2011;375:3801–3803. doi: 10.1016/j.physleta.2011.08.023
[12] Shen Y, Liu H, Fu J, et al. Double rainbow trapping of light in one-dimensional chirped metallic–dielectric photonic crystals. J Opt Soc Am B. 2011;28:2444–2447. doi: 10.1364/JOSAB.28.002444
[13] Kurt H, Yilmaz D. Rainbow trapping using chirped all-dielectric periodic structures. Appl Phys B. 2013;110:411–417. doi: 10.1007/s00340-012-5270-8
[14] Shen Q, Shen L, Min W, et al. Trapping a magnetic rainbow by using a one-way magnetostatic-like mode. Opt Mater Express. 2019;9:4399–4408. doi: 10.1364/OME.9.004399
[15] Elshahat S, Lu C. Bidirectional rainbow trapping in 1-D chirped topological photonic crystal. Front Phys. 2022;10:29. doi: 10.3389/fphy.2022.831203
[16] Davies B, Chaplain G, Starkey T, et al. Graded quasiperiodic metamaterials perform fractal rainbow trapping. Phys Rev Lett. 2023;131:177001. doi: 10.1103/PhysRevLett.131.177001
[17] Ding F, Mao Y, Shen J, et al. Simultaneous slow light and sound rainbow trapping in phoxonic crystals. Opt Lett. 2022;47:5650–5653. doi: 10.1364/OL.475372
[18] Chen J, Qin Q, Peng C, et al. Slow light rainbow trapping in a uniformly magnetized gyromagnetic photonic crystal waveguide. Front Mater. 2021;8:Volume 8–2021. doi: 10.3389/fmats.2021.728991
[19] Baba T. Slow light in photonic crystals. Nat Photonics. 2008;2:465. doi: 10.1038/nphoton.2008.146
[20] Elshahat S, Abood I, Khan K, et al. Five-line photonic crystal waveguide for optical buffering and data interconnection of picosecond pulse. J Lightwave Technol. 2019;37:788–798. doi: 10.1109/JLT.2018.2881121

[21] Elshahat S, Abood I, Liang Z, et al. Sporadic-slot photonic-crystal waveguide for all-optical buffers with low-dispersion, distortion, and insertion loss. IEEE Access. 2020;8:77689–77700. doi: 10.1109/ACCESS.2020.2986082
[22] Elshahat S, Abood I, Liang Z, et al. Dispersion engineering of W2 steeple-house-defect waveguide photonic crystal. Results Phys. 2020;19:103547. doi: 10.1016/j.rinp.2020.103547
[23] Krauss TF. Why do we need slow light? Nat Photonics. 2008;2:448. doi: 10.1038/nphoton.2008.139
[24] Khurgin JB, Tucker RS. Slow light: science and applications. Boca Raton: CRC press; 2018.
[25] Li J, White TP, O'Faolain L, et al. Systematic design of flat band slow light in photonic crystal waveguides. Opt Express. 2008;16:6227–6232. doi: 10.1364/OE.16.006227
[26] Tsakmakidis KL, Shen L, Schulz SA, et al. Breaking Lorentz reciprocity to overcome the time-bandwidth limit in physics and engineering. Science. 2017;356:1260–1264. doi: 10.1126/science.aam6662
[27] Abood I, Elshahat S, Khan K, et al. Slow light with high normalized delay-bandwidth product in low-dispersion photonic-crystal coupled-cavity waveguide. Optics Commun. 2019;439:181–186. doi: 10.1016/j.optcom.2019.01.063
[28] Tsakmakidis KL, Baskourelos K, Stefański T. Topological, nonreciprocal, and multiresonant slow light beyond the time-bandwidth limit. Appl Phys Lett. 2021;119. doi: 10.1063/5.0068285
[29] Giden IH, Kurt H, Turduev M, etal. Compact rainbow trapping and demultiplexing by photonic crystal waveguides. In: 2014 IEEE Photonics Conference; San Diego, CA, USA; 2014.
[30] Fanglong W, Yizhou S, Yanlong X, et al. Rainbow trapping of flexural waves and its application in energy harvesting. Chin J Theor Appl Mech. 2022;54:2695–2707.
[31] Gan Q, Ding YJ, Bartoli FJ. "Rainbow" trapping and releasing at telecommunication wavelengths. Phys Rev Lett. 2009;102:056801. doi: 10.1103/PhysRevLett.102.056801
[32] Wang G, Lu H, Liu X. Gain-assisted trapping of light in tapered plasmonic waveguide. Opt Lett. 2013;38:558–560. doi: 10.1364/OL.38.000558
[33] Montazeri AO, Fang Y, Sarrafi P, et al. Rainbow-trapping by adiabatic tuning of intragroove plasmon coupling. Opt Express. 2016;24:26745–26755. doi: 10.1364/OE.24.026745
[34] Dixon K, Montazeri AO, Shayegannia M, et al. Tunable rainbow light trapping in ultrathin resonator arrays. Light Sci Appl. 2020;9:194. doi: 10.1038/s41377-020-00428-y
[35] Kazemi-Zanjani N, Shayegannia M, Prinja R, et al. Multiwavelength surface-enhanced Raman spectroscopy using rainbow trapping in width-graded plasmonic gratings. Adv Optical Mater. 2018;6:1701136. doi: 10.1002/adom.201701136
[36] Zeineddine A, Shayegannia M, Kherani NP, et al. Exploiting graded triangular gratings for optimal nano-focusing: a novel approach to enhance SERS efficiency. APL Photonics. 2024;9. doi: 10.1063/5.0195141
[37] Liu K, He S. Truly trapped rainbow by utilizing nonreciprocal waveguides. Sci Rep. 2016;6:30206. doi: 10.1038/srep30206
[38] Lu H, Zeng C, Zhang Q, et al. Graphene-based active slow surface plasmon polaritons. Sci Rep. 2015;5:8443. doi: 10.1038/srep08443
[39] Ghaderian P, Habibzadeh-Sharif A. Rainbow trapping and releasing in graded grating graphene plasmonic waveguides. Opt Express. 2021;29:3996–4009. doi: 10.1364/OE.414982

[40] Xu Z, Shi J, Davis RJ, et al. Rainbow trapping with long oscillation lifetimes in gradient magnetoinductive metasurfaces. Phys Rev Appl. 2019;12:024043. doi: 10.1103/PhysRevApplied.12.024043
[41] Li J, Hu G, Shi L, et al. Full-color enhanced second harmonic generation using rainbow trapping in ultrathin hyperbolic metamaterials. Nat Commun. 2021;12:6425. doi: 10.1038/s41467-021-26818-3
[42] Xu J, Xiao S, He P, et al. Realization of broadband truly rainbow trapping in gradient-index metamaterials. Opt Express. 2022;30:3941–3953. doi: 10.1364/OE.447874
[43] Jang MS, Atwater H. Plasmonic rainbow trapping structures for light localization and spectrum splitting. Phys Rev Lett. 2011;107:207401. doi: 10.1103/PhysRevLett.107.207401
[44] Chen L, Wang GP, Gan Q, et al. Rainbow trapping and releasing by chirped plasmonic waveguides at visible frequencies. Appl Phys Lett. 2010;97:153115. doi: 10.1063/1.3502487
[45] Chen L, Zhang T, Li X, et al. Plasmonic rainbow trapping by a graphene monolayer on a dielectric layer with a silicon grating substrate. Opt Express. 2013;21:28628–28637. doi: 10.1364/OE.21.028628
[46] Farid S, Dixon K, Shayegannia M, et al. Rainbows at the end of subwavelength discontinuities: plasmonic light trapping for sensing applications. Adv Optical Mater. 2021;9:2100695. doi: 10.1002/adom.202100695
[47] Gan Q, Gao Y, Wagner K, etal. Experimental verification of the rainbow trapping effect in adiabatic plasmonic gratings. Proc Natl Acad Sci USA. 2011;108(13):5169–5173.
[48] Hu H, Ji D, Zeng X, et al. Rainbow trapping in hyperbolic metamaterial waveguide. Sci Rep. 2013;3:1249. doi: 10.1038/srep01249
[49] Liu Y, Wang Y, Han G, et al. Engineering rainbow trapping and releasing in ultrathin THz plasmonic graded metallic grating strip with thermo-optic material. Opt Express. 2017;25:1278–1287. doi: 10.1364/OE.25.001278
[50] Xu J, Xiao S, Wu C, et al. Broadband one-way propagation and rainbow trapping of terahertz radiations. Opt Express. 2019;27:10659–10669. doi: 10.1364/OE.27.010659
[51] Yin X, Zhang T, Chen L, et al. Plasmonic rainbow trapping by a silica–graphene–silica on a sloping silicon substrate. J Lightwave Technol. 2014;32:4193–4198. doi: 10.1109/JLT.2014.2350481
[52] Yin X, Zhang T, Chen L, et al. Plasmonic rainbow trapping by a silica–graphene–silica on a sloping silicon substrate. J Lightwave Technol. 2014;32:3591–3596. doi: 10.1109/JLT.2014.2350481
[53] Liu Y, Kanyang R, Han G, et al. Rainbow trapping in highly doped silicon graded grating strip at the terahertz range. IEEE Photonics J. 2018;10:1–9. doi: 10.1109/JPHOT.2018.2816566
[54] He C, Wu H, Feng Y, et al. Dynamic modulation of slow light rainbow trapping and releasing in a tapered waveguide based on low-symmetric photonic crystals. Results Phys. 2021;28:104592. doi: 10.1016/j.rinp.2021.104592
[55] Giden IH, Mahariq I. Optical demultiplexing via rainbow trapping in graded-index photonic crystal waveguides. Opt Quant Electron. 2023;56:170. doi: 10.1007/s11082-023-05768-8
[56] Hayran Z, Kurt H, Staliunas K. Rainbow trapping in a chirped three-dimensional photonic crystal. Sci Rep. 2017;7:3046. doi: 10.1038/s41598-017-03454-w
[57] Neşeli B, Bor E, Kurt H, et al. Rainbow trapping in a tapered photonic crystal waveguide and its application in wavelength demultiplexing effect. J Opt Soc Am B. 2020;37:1249–1256. doi: 10.1364/JOSAB.388374

[58] Soliman SE, Abood I, Lu C. Robust multi-mode rainbow trapping with ultra-high-Q Fano resonances. Opt Express. 2024;32:1010–1019. doi: 10.1364/OE.512258

[59] Sharma S, Mondal A, Das R. Infrared rainbow trapping via optical Tamm modes in an one-dimensional dielectric chirped photonic crystals. Opt Lett. 2021;46:4566–4569. doi: 10.1364/OL.437958

[60] Zhu J, Chen Y, Zhu X, et al. Acoustic rainbow trapping. Sci Rep. 2013;3:1728. doi: 10.1038/srep01728

[61] Lee S-S, Jang J-Y, Song K. Enhanced acoustic attenuation in a coiled meta-silencer: broadband low-frequency noise control through rainbow trapping. Mech Syst & Signal Process. 2025;222:111744. doi: 10.1016/j.ymssp.2024.111744

[62] Xu B-Q, Wu J, Lu W, et al. Transmission and rainbow trapping of acoustic waves in a fluid medium using gradient-index superlattices. J Appl Phys. 2021;129. doi: 10.1063/5.0040507

[63] Wu H-W, Yin Y-Q, Sheng Z-Q, et al. Multiband omnidirectional ventilated acoustic barriers based on localized acoustic rainbow trapping. Phys Rev Appl. 2021;15:054033. doi: 10.1103/PhysRevApplied.15.054033

[64] Zhao L, Zhou S. Compact acoustic rainbow trapping in a bioinspired spiral array of graded locally resonant metamaterials. Sensors. 2019;19:788. doi: 10.3390/s19040788

[65] Lu Y, Dong D, Li X, et al. Acoustic rainbow trapping in cylindrical spoof waveguide. Appl Acoust. 2025;231:110502. doi: 10.1016/j.apacoust.2024.110502

[66] Tian Z, Yu L. Rainbow trapping of ultrasonic guided waves in chirped phononic crystal plates. Sci Rep. 2017;7:40004. doi: 10.1038/srep40004

[67] De Ponti JM, Iorio L, Ardito R, et al. Graded elastic meta-waveguides for rainbow reflection, trapping and mode conversion. EPJ Appl Metamat. 2022;9:6. doi: 10.1051/epjam/2022004

[68] Wang B, Huang Y, Zhou W, et al. Metamaterial beam for flexural wave resonance rainbow trapping and piezoelectric energy harvesting. J Appl Phys. 2021;129. doi: 10.1063/5.0040029

[69] Skelton E, et al. The multi-physics metawedge: graded arrays on fluid-loaded elastic plates and the mechanical analogues of rainbow trapping and mode conversion. New J Phys. 2018;20:053017. doi: 10.1088/1367-2630/aabecf

[70] De Ponti JM, Iorio L, Riva E, et al. Selective mode conversion and rainbow trapping via graded elastic waveguides. Phys Rev Appl. 2021;16:034028. doi: 10.1103/PhysRevApplied.16.034028

[71] Alshaqaq M, Sugino C, Erturk A. Programmable rainbow trapping and band-gap enhancement via spatial group-velocity tailoring in elastic metamaterials. Phys Rev Appl. 2022;17:L021003. doi: 10.1103/PhysRevApplied.17.L021003

[72] Ellouzi C, Zabihi A, Gormley L, et al. Experimental demonstration of rainbow trapping of elastic waves in two-dimensional axisymmetric phononic crystal plates. J Acoust Soc Am. 2024;155:1759–1766. doi: 10.1121/10.0025179

[73] Tian F, Wang Y, Huang W, et al. Ultra-compact topological photonic crystal rainbow nanolasers operating in the 1550 nm telecom band with wavelength-scale mode volumes. arxiv Prepr arXiv:2411.11009, 2024.

[74] Chen JJ, Yang Q-S, Huo S-Y, et al. Multidimensional rainbow trapping of sound in the second-order topological sonic crystals. Physica Status Solidi (B). 2024:2400200. doi: 10.1002/pssb.202400200

[75] Chen Y, Fan L, Zhu J, et al. Rainbow energy harvesting using a high-order topological meta-device. Nano Energy. 2024;127:109722. doi: 10.1016/j.nanoen.2024.109722

[76] AbdelAll N, Almokhtar M, Khouqeer G, et al. Rainbow trapping with engineered topological corner states and cavities in photonic crystals. Adv Quantum Tech. 2024:2400050. doi: 10.1002/qute.202400050

[77] AbdelAll N, et al. Realizing the topological rainbow based on cavity-coupled topological edge state. Optics & Laser Technol. 2024;171:110351. doi: 10.1016/j.optlastec.2023.110351

[78] Elshahat S, Zhang H, Lu C. Topological rainbow based on coupling of topological waveguide and cavity. Opt Express. 2023;31:20187–20199. doi: 10.1364/OE.493182

[79] Wang X, Zhao W, Elshahat S, et al. Topological rainbow trapping based on gradual valley photonic crystals. Front Phys. 2023;11:11. doi: 10.3389/fphy.2023.1141997

[80] Lu C, Wang C, Xiao M, et al. Topological rainbow concentrator based on synthetic dimension. Phys Rev Lett. 2021;126:113902. doi: 10.1103/PhysRevLett.126.113902

[81] Bu X, Huang H, Chen J. Topological rainbow trapping of shear horizontal waves in a phononic crystal plate with tapered surface. Phys Scr. 2024;99:075915. doi: 10.1088/1402-4896/ad505b

[82] Liu C, Zhang Z, Liao D, et al. Rainbow trapping for sound waves in one-dimensional topological insulator. Appl Phys Lett. 2023;123. doi: 10.1063/5.0155714

[83] Xu J, He P, Feng D, et al. Slow wave and truly rainbow trapping in a one-way terahertz waveguide. Opt Express. 2021;29:11328–11341. doi: 10.1364/OE.422274

[84] Abood I, Elshahat S, Ouyang Z. High fi gure of merit optical buffering in coupled-slot slab photonic crystal waveguide with ionic liquid. Nanomaterials. 2020;10:1742. doi: 10.3390/nano10091742

[85] Abood I, Elshahat S, Ouyang Z. High buffering capability of silicon-polymer photonic-crystal coupled cavity waveguide. Waves Random & Complex Media. 2021;33:296–311. doi: 10.1080/17455030.2021.1879406

[86] Elshahat S, Abood I, Khan K, et al. High-capability micro-optical buffer based on coupled hexagonal cavity in photonic crystal waveguide. Appl Nanosci. 2019;9:1963–1970. doi: 10.1007/s13204-019-00999-2

[87] Elshahat S, Abood I, Liang Z, et al. Elongated-hexagonal photonic crystal for buffering, sensing, and modulation. Nanomaterials. 2021;11:809. doi: 10.3390/nano11030809

[88] Elshahat S, Esmail MSM, Yuan H, et al. Broadband multiple topological rainbows. Annalen der Phys. 2022;534:2200137. doi: 10.1002/andp.202200137

[89] Ni X, Wu Y, Chen Z-G, et al. Acoustic rainbow trapping by coiling up space. Sci Rep. 2014;4:7038. doi: 10.1038/srep07038

[90] Zhou C, Yuan B, Cheng Y, et al. Precise rainbow trapping for low-frequency acoustic waves with micro Mie resonance-based structures. Appl Phys Lett. 2016;108. doi: 10.1063/1.4941664

[91] Arreola-Lucas A, Báez G, Cervera F, etal. Mechanical rainbow trapping and Bloch oscillations in structured elastic beams. arxiv Prepr arXiv:1707.06558, 2017. doi:https://doi.org/10.48550/arXiv.1707.06558.

[92] Arreola-Lucas A, Báez G, Cervera F, et al. Experimental evidence of rainbow trapping and Bloch Oscillations of torsional waves in chirped metallic beams. Sci Rep. 2019;9:1860. doi: 10.1038/s41598-018-37842-7

[93] Chaplain GJ, Pajer D, De Ponti JM, et al. Delineating rainbow reflection and trapping with applications for energy harvesting. New J Phys. 2020;22:063024. doi: 10.1088/1367-2630/ab8cae

[94] Tang X-L, Zhang X-Q, Ma T-X, et al. Topological rainbow trapping and broadband piezoelectric energy harvesting of acoustic waves in gradient phononic crystals with coupled interfaces. Appl Acoust arXiv:2404.09160, 2024;233:110630. doi: 10.1016/j.apacoust.2025.110630

[95] Chaplain GJ, De Ponti JM, Aguzzi G, et al. Topological rainbow trapping for elastic energy harvesting in graded Su-Schrieffer-heeger systems. Phys Rev Appl. 2020;14:054035. doi: 10.1103/PhysRevApplied.14.054035
[96] Lu C, Sun Y-Z, Wang C, et al. On-chip nanophotonic topological rainbow. Nat Commun. 2022;13:2586. doi: 10.1038/s41467-022-30276-w
[97] Liang L, Zhou X, Hu J-H, et al. Rainbow trapping based on higher-order topological corner modes. Opt Lett. 2022;47:1454–1457. doi: 10.1364/OL.451770
[98] Zhao W, Zheng Y, Lu C. Topological rainbow trapping based on non-hermitian twisted piecing photonic crystals. Photon Res. 2022;10:2728–2733. doi: 10.1364/PRJ.470354
[99] Zhang W-J, Mo H-C, Chen W-J, et al. Observation of gapless corner modes of photonic crystal slabs in synthetic translation dimensions. Photon Res. 2024;12:444–455. doi: 10.1364/PRJ.506167
[100] Liao D, Liu Y, Zhang Z, et al. Synthesizing topological acoustic rainbow trapping at deep-subwavelength corners. Sci Bull. 2023;68:1744–1747. doi: 10.1016/j.scib.2023.07.016
[101] Tang X-L, Ma T-X, Wang Y-S. Topological rainbow trapping and acoustic energy amplification in two-dimensional gradient phononic crystals. Appl Phys Lett. 2023;122. doi: 10.1063/5.0138982
[102] Yuan W, Zhang Y, Pan Y, et al. Topological rainbow trapping, concentration and guiding in graded elastic valley phononic crystal plate. Eng Struct. 2024;304:117596. doi: 10.1016/j.engstruct.2024.117596
[103] Wang G, Wei Y, Chen Z, et al. Controllable subwavelength topological rainbow trapping in water-filling acoustic metamaterials. Appl Acoust. 2023;207:109366. doi: 10.1016/j.apacoust.2023.109366
[104] Noh J, Huang S, Chen KP, et al. Observation of photonic topological valley hall edge states. Phys Rev Lett. 2018;120:063902. doi: 10.1103/PhysRevLett.120.063902
[105] Poo Y, Wu R-X, Lin Z, et al. Experimental realization of self-guiding unidirectional electromagnetic edge states. Phys Rev Lett. 2011;106:093903. doi: 10.1103/PhysRevLett.106.093903
[106] Ma T, Shvets G. Scattering-free edge states between heterogeneous photonic topological insulators. Phys Rev B. 2017;95:165102. doi: 10.1103/PhysRevB.95.165102
[107] Xie B-Y, Wang H-F, Wang H-X, et al. Second-order photonic topological insulator with corner states. Phys Rev B. 2018;98:205147. doi: 10.1103/PhysRevB.98.205147
[108] Xie B-Y, Su G-X, Wang H-F, et al. Visualization of higher-order topological insulating phases in two-dimensional dielectric photonic crystals. Phys Rev Lett. 2019;122:233903. doi: 10.1103/PhysRevLett.122.233903
[109] Li M, Zhirihin D, Gorlach M, et al. Higher-order topological states in photonic kagome crystals with long-range interactions. Nat Photonics. 2020;14:89–94. doi: 10.1038/s41566-019-0561-9
[110] Wu L-H, Hu X. Scheme for achieving a topological photonic crystal by using dielectric material. Phys Rev Lett. 2015;114:223901. doi: 10.1103/PhysRevLett.114.223901
[111] Chen Z-G, Mei J, Sun X-C, et al. Multiple topological phase transitions in a gyromagnetic photonic crystal. Phys Rev A. 2017;95:043827. doi: 10.1103/PhysRevA.95.043827
[112] Chan H-C, Guo G-Y. Tuning topological phase transitions in hexagonal photonic lattices made of triangular rods. Phys Rev B. 2018;97:045422. doi: 10.1103/PhysRevB.97.045422
[113] Wang Q, Xue H, Zhang B, et al. Observation of protected photonic edge states induced by real-space topological lattice defects. Phys Rev Lett. 2020;124:243602. doi: 10.1103/PhysRevLett.124.243602

[114] Peterson CW, Li T, Jiang W, et al. Trapped fractional charges at bulk defects in topological insulators. Nature. 2021;589:376–380. doi: 10.1038/s41586-020-03117-3
[115] Noh J, Benalcazar WA, Huang S, et al. Topological protection of photonic mid-gap defect modes. Nat Photonics. 2018;12:408–415. doi: 10.1038/s41566-018-0179-3
[116] Skirlo SA, Lu L, Igarashi Y, et al. Experimental observation of large Chern numbers in photonic crystals. Phys Rev Lett. 2015;115:253901. doi: 10.1103/PhysRevLett.115.253901
[117] Skirlo SA, Lu L, Soljačić M. Multimode one-way waveguides of large Chern numbers. Phys Rev Lett. 2014;113:113904. doi: 10.1103/PhysRevLett.113.113904
[118] Lu L, Joannopoulos JD, Soljačić M. Topological states in photonic systems. Nat Phys. 2016;12:626–629. doi: 10.1038/nphys3796
[119] Elshahat S, Abood I, Khan K, et al. Ultra-wideband slow light transmission with high normalized delay bandwidth product in W3 photonic crystal waveguide. Superlattices & Microstruct. 2018;121:45–54. doi: 10.1016/j.spmi.2018.07.025
[120] Figotin A, Vitebskiy I. Frozen light in photonic crystals with degenerate band edge. Phys Rev E. 2006;74:066613. doi: 10.1103/PhysRevE.74.066613
[121] Zhao J, Wu X, Zhang D, et al. Amber rainbow ribbon effect in broadband optical metamaterials. Nat Commun. 2024;15:2613. doi: 10.1038/s41467-024-46914-4
[122] Anderson SP, Shroff AR, Fauchet PM, et al. Slow light with photonic crystals for on-chip optical interconnects. Adv Optical Technol. 2008;2008:1–12. doi: 10.1155/2008/293531
[123] Chao Z, Yan H, Xiao-Yu M, et al. Slow light by two-dimensional photonic crystal waveguides. Chin Phys Lett. 2009;26:074216. doi: 10.1088/0256-307X/26/7/074216
[124] Chen J, Liang W, Li Z-Y. Broadband dispersionless topological slow light. Opt Lett. 2020;45:4964–4967. doi: 10.1364/OL.401650
[125] Elshahat S, Abood I, Khan K, etal. Ultra-high group index slow light with optical buffering performance in photonic crystal waveguide coupled with cavity. In: Proc. SPIE/COS Photonics Asia 2018; Quantum and Nonlinear Optics V 2018 Nov 9. Vol. 10825. Beijing, China: SPIE; 2018. doi:https://doi.org/10.1117/12.2500088.
[126] Elshahat S, Abood I, Liang Z, et al. Futuristic elongated-hexagonal photonic crystal waveguide for slow light. Optics Commun. 2020;474:126082. doi: 10.1016/j.optcom.2020.126082
[127] Elshahat S, Khan K, Yadav A, et al. Slow-light transmission with high group index and large normalized delay bandwidth product through successive defect rods on intrinsic photonic crystal waveguide. Optics Commun. 2018;418:73–79. doi: 10.1016/j.optcom.2018.02.063
[128] Hamachi Y, Kubo S, Baba T. Slow light with low dispersion and nonlinear enhancement in a lattice-shifted photonic crystal waveguide. Opt Lett. 2009;34:1072–1074. doi: 10.1364/OL.34.001072
[129] Hao R, Peng X-L, Li E-P, et al. Improved slow light capacity in graphene-based waveguide. Sci Rep. 2015;5:15335. doi: 10.1038/srep15335
[130] Liu L, Wang Y, Li M, et al. Slow light in topological coupled-corner-state waveguide. J Phys D: Appl Phys. 2022;55:335104. doi: 10.1088/1361-6463/ac7113
[131] Yan S, Zhu X, Frandsen LH, et al. Slow-light-enhanced energy efficiency for graphene microheaters on silicon photonic crystal waveguides. Nat Commun. 2017;8:14411. doi: 10.1038/ncomms14411
[132] Khanikaev AB, Hossein Mousavi S, Tse W-K, et al. Photonic topological insulators. Nat Mater. 2013;12:233–239. doi: 10.1038/nmat3520
[133] Khanikaev AB, Shvets G. Two-dimensional topological photonics. Nat Photonics. 2017;11:763–773. doi: 10.1038/s41566-017-0048-5

[134] Lu L, Joannopoulos JD, Soljačić M. Topological photonics. Nat Photonics. 2014;8:821–829. doi: 10.1038/nphoton.2014.248
[135] Ota Y, Takata K, Ozawa T, et al. Active topological photonics. Nanophotonics. 2020;9:547–567. doi: 10.1515/nanoph-2019-0376
[136] Ozawa T, Price HM, Amo A, et al. Topological photonics. Rev Mod Phys. 2019;91:015006. doi: 10.1103/RevModPhys.91.015006
[137] Wu X, Meng Y, Tian J, et al. Direct observation of valley-polarized topological edge states in designer surface plasmon crystals. Nat Commun. 2017;8:1–9. doi: 10.1038/s41467-017-01515-2
[138] Mei J, Wu Y, Chan CT, et al. First-principles study of Dirac and Dirac-like cones in phononic and photonic crystals. Phys Rev B. 2012;86:035141. doi: 10.1103/PhysRevB.86.035141
[139] Tang G-J, Chen X-D, Shi F-L, et al. Frequency range dependent topological phases and photonic detouring in valley photonic crystals. Phys Rev B. 2020;102:174202. doi: 10.1103/PhysRevB.102.174202
[140] Tian Z, Shen C, Li J, et al. Dispersion tuning and route reconfiguration of acoustic waves in valley topological phononic crystals. Nat Commun. 2020;11:762. doi: 10.1038/s41467-020-14553-0
[141] Chen T, Xia B, Yu D, et al. Robust enhanced acoustic sensing via gradient phononic crystals. Phys Lett A. 2024;493:129242. doi: 10.1016/j.physleta.2023.129242
[142] Guan A-Y, Yang Z-Z, Yang W-J, et al. Controlling sound wave propagation in topological crystalline insulators and rainbow-trapping. Phys Rev Appl. 2022;18:044054. doi: 10.1103/PhysRevApplied.18.044054
[143] Yang Q-S, Chen R-H, Huo S-Y. Dimensional hierarchy of acoustic topological rainbow trapping in two-dimensional phononic crystals. Mater Today Commun. 2024;40:110060. doi: 10.1016/j.mtcomm.2024.110060
[144] Wang G, Guan Y, Chen Z, et al. New topological rainbow trapping approach for phononic beam-foundation systems. J Phys D: Appl Phys. 2023;56:385309. doi: 10.1088/1361-6463/acdc38
[145] Ni X, Yves S, Krasnok A, et al. Topological metamaterials. Chem Rev. 2023;123:7585–7654. doi: 10.1021/acs.chemrev.2c00800
[146] Kartashov YV, Astrakharchik GE, Malomed BA, et al. Frontiers in multidimensional self-trapping of nonlinear fields and matter. Nat Rev Phys. 2019;1:185–197. doi: 10.1038/s42254-019-0025-7
[147] Wuestner S, et al. Gain in negative-index metamaterials and slow-light waveguides. In: Metamaterials: fundamentals and applications III. SPIE; 2010.
[148] Wuestner S, Pusch A, Tsakmakidis KL, et al. Overcoming losses with gain in a negative refractive index metamaterial. Phys Rev Lett. 2010;105:127401. doi: 10.1103/PhysRevLett.105.127401
[149] Tsakmakidis KL, Hess O. Extreme control of light in metamaterials: complete and loss-free stopping of light. Physica B: Condens Matter. 2012;407:4066–4069. doi: 10.1016/j.physb.2012.01.093
[150] Kumar A, Gupta M, Pitchappa P, et al. Active ultrahigh- Q (0.2 × 10 6) THz topological cavities on a chip. Adv Mater. 2022;34:2202370. doi: 10.1002/adma.202202370
[151] Zheng Z, Chen Y, Wang F, et al. High-$ Q $ bound state in the continuum cavity enabled by high-order topological charge. In: IEEE Photonics Journal; 2024.
[152] Huang L, Jin R, Zhou C, et al. Ultrahigh-Q guided mode resonances in an all-dielectric metasurface. Nat Commun. 2023;14:3433. doi: 10.1038/s41467-023-39227-5
[153] Chen Y, Lan Z, Su Z, et al. Inverse design of photonic and phononic topological insulators: a review. Nanophotonics. 2022;11:4347–4362. doi: 10.1515/nanoph-2022-0309

[154] Wang F, Jensen JS, Sigmund O. Robust topology optimization of photonic crystal waveguides with tailored dispersion properties. J Opt Soc Am B. 2011;28:387–397. doi: 10.1364/JOSAB.28.000387

[155] Feng C, et al. Ultra-low-power tunable topological photonic filter on hybrid integrated lithium tantalite and silicon platform. Laser & Photonics Rev. 2024:2300360. doi: 10.1002/lpor.202300360

[156] Makwana M, Wiltshaw R, Guenneau S, et al. Hybrid topological guiding mechanisms for photonic crystal fibers. Opt Express. 2020;28:30871–30888. doi: 10.1364/OE.398559

[157] Wu Y, Li C, Hu X, et al. Applications of topological photonics in integrated photonic devices. Adv Optical Mater. 2017;5:1700357. doi: 10.1002/adom.201700357

[158] Zhang Z, Tian Y, Cheng Y, et al. Topological acoustic delay line. Phys Rev Appl. 2018;9:034032. doi: 10.1103/PhysRevApplied.9.034032

[159] Shi Y, Zhang Y, Wan Y, et al. Silicon photonics for high-capacity data communications. Photon Res. 2022;10:A106–A134. doi: 10.1364/PRJ.456772

[160] Bamiedakis N, Williams KA, Penty RV et al. Integrated and hybrid photonics for high-performance interconnects. Optical Fiber Telecommun Volume VIA: Components & Subsystems. 2013:377–416.

[161] Tong XC. Advanced materials for integrated optical waveguides. Vol. 46. Springer; 2014.

[162] Rumley S, Nikolova D, Hendry R, et al. Silicon photonics for exascale systems. J Lightwave Technol. 2015;33:547–562. doi: 10.1109/JLT.2014.2363947

[163] Lee G, Lee S-J, Rho J, et al. Acoustic and mechanical metamaterials for energy harvesting and self-powered sensing applications. Mater Today Energy. 2023;37:101387. doi: 10.1016/j.mtener.2023.101387

[164] De Ponti JM, Colombi A, Ardito R, et al. Graded elastic metasurface for enhanced energy harvesting. New J Phys. 2020;22:013013. doi: 10.1088/1367-2630/ab6062

[165] Pantuso S. Acoustic topological states on RF piezo-electric MEMS technology and possible sensing appli-cations. Politecnico di Torino; 2025.

[166] Gormley LA. Rainbow trapping effect in 2D axisymmetric broadband acoustic energy harvesters. Rowan University; 2021.

[167] Santini J, Sugino C, Riva E, et al. Harnessing rainbow trapping via hybrid electromechanical metastructures for enhanced energy harvesting and vibration attenuation. J Appl Phys. 2022;132. doi: 10.1063/5.0090258

[168] Mao X-R, Shao Z-K, Luan H-Y, et al. Magic-angle lasers in nanostructured moiré superlattice. Nat Nanotechnol. 2021;16:1099–1105. doi: 10.1038/s41565-021-00956-7

[169] Tsakmakidis KL. Stopped-light nanolasing in optical magic-angle graphene. Nat Nanotechnol. 2021;16:1048–1049. doi: 10.1038/s41565-021-00960-x

[170] Luan H-Y, Ouyang Y-H, Zhao Z-W, et al. Reconfigurable moiré nanolaser arrays with phase synchronization. Nature. 2023;624:282–288. doi: 10.1038/s41586-023-06789-9

[171] Ouyang Y-H, Luan H-Y, Zhao Z-W, et al. Singular dielectric nanolaser with atomic-scale field localization. Nature. 2024;632:287–293. doi: 10.1038/s41586-024-07674-9